



Published in final edited form as:

Biomaterials. 2011 January ; 32(1): 10–18. doi:10.1016/j.biomaterials.2010.08.073.

The Biocompatibility of Titanium Cardiovascular Devices Seeded With Autologous Blood-Derived Endothelial Progenitor Cells:

EPC-Seeded Antithrombotic Ti Implants

Hardean E. Achneck, M.D.^{1,*}, Ryan M. Jamiolkowski, B.A.¹, Alexandra E. Jantzen, B.S.², Justin Haseltine², Whitney O. Lane, B.S.³, Jessica Huang, B.S.³, Lauren J. Galinat², Michael J. Serpe, Ph.D.⁴, Fu-Hsiung Lin, Ph.D.¹, Madison Li, B.S.E.², Amar Parikh, B.A.³, Liqiao Ma, B.S.³, Tao Chen, Ph.D.⁵, Bantayehu Sileshi, M.D.¹, Carmelo A. Milano, M.D.⁶, Charles S. Wallace, Ph.D.², Thomas V. Stabler, M.S.⁷, Jason D. Allen, Ph.D.⁷, George A. Truskey, Ph.D.², and Jeffrey H. Lawson, M.D., Ph.D.^{1,8,9}

¹Department of Surgery, Division of General Surgery, Duke University Medical Center, DUMC Box 2622, Durham, North Carolina 27710, USA

²Department of Biomedical Engineering, Duke University, 136 Hudson Hall, Box 90281, Durham, NC 27708, USA

³Department of Biology, Duke University, Box 90338, Durham, NC 27708, USA

⁴Department of Chemistry, Duke University, 124 Science Drive, Box 90354, Durham, NC 27708, USA

⁵Departments of Mechanical Engineering and Material Science, 144 Hudson Hall, Duke University, Box 90300, Durham, NC 27708, USA

⁶Department of Surgery, Division of Cardiovascular and Thoracic Surgery, Duke University Medical Center, Box 3043, Durham, NC 27710, USA

⁷Department of Medicine, Duke University, Box 3022, Durham, NC 27710, USA

⁸Department of Pathology, Duke University, Durham, NC 27710, USA

⁹Department of Surgery, Section of Vascular Surgery, Duke University Medical Center, DUMC Box 2622, Research Drive, Durham, North Carolina 27710, USA

Abstract

Implantable and extracorporeal cardiovascular devices are commonly made from titanium (Ti) (e.g. Ti-coated Nitinol stents and mechanical circulatory assist devices). Endothelializing the

© 2010 Elsevier Ltd. All rights reserved.

*Corresponding author: Hardean E. Achneck, M.D.¹, Department of Surgery, Division of General Surgery, Duke University Medical Center, DUMC Box 2622, Durham, North Carolina 27710, USA; hardean.achneck@duke.edu, Phone: 919-668-6113, Fax: 919-668-6113.

Publisher's Disclaimer: This is a PDF file of an unedited manuscript that has been accepted for publication. As a service to our customers we are providing this early version of the manuscript. The manuscript will undergo copyediting, typesetting, and review of the resulting proof before it is published in its final citable form. Please note that during the production process errors may be discovered which could affect the content, and all legal disclaimers that apply to the journal pertain.

blood-contacting Ti surfaces of these devices would provide them with an antithrombogenic coating that mimics the native lining of blood vessels and the heart. We evaluated the viability and adherence of peripheral blood-derived porcine endothelial progenitor cells (EPCs), seeded onto thin Ti layers on glass slides under static conditions and after exposure to fluid shear stresses. EPCs attached and grew to confluence on Ti in serum-free medium, without preadsorption of proteins. After attachment to Ti for 15 min, less than 5 % of the cells detached at a shear stress of 100 dyne/cm². Confluent monolayers of EPCs on smooth Ti surfaces (R_q of 10 nm), exposed to 15 or 100 dyne/cm² for 48 hours, aligned and elongated in the direction of flow and produced nitric oxide dependent on the level of shear stress. EPC-coated Ti surfaces had dramatically reduced platelet adhesion when compared to uncoated Ti surfaces. These results indicate that peripheral blood-derived EPCs adhere and function normally on Ti surfaces. Therefore EPCs may be used to seed cardiovascular devices prior to implantation to ameliorate platelet activation and thrombus formation.

Keywords

Biocompatibility; Cell adhesion; Progenitor cell; Titanium; Thrombogenicity; Endothelialisation

1. Introduction

Implantable and extracorporeal blood-contacting medical devices are commonly engineered of titanium (Ti) because of its superior physiochemical properties. Mechanical circulatory assist devices (MCADs) utilize Ti for its corrosion resistance and very high strength-to-weight ratio. MCADs benefit patients with severe heart failure refractory to medical treatment. Because of the limited supply for heart transplants, with less than 2,200 donor organs available each year in the US, it is estimated that 250,000 adult patients with end-stage heart failure per year would benefit from MCAD implantation as either a bridge to heart transplantation or as a permanent destination therapy [1].

Other examples of implantable vascular devices, which utilize Ti, are self-expanding Nitinol stents. In these stents, the combination of titanium with nickel endows them with a superelasticity and thermal shape memory rendering them resistant to compression at body temperature and provides for a continuous radial pressure against a stented vessel wall [2]. To prevent nickel ions from leaching into the bloodstream, the manufacturers of Nitinol stents produce a barrier layer of only Ti on the outer blood-contacting surface of the stent [3]. Nitinol stents are increasingly being employed in the treatment of patients with cerebral and peripheral vascular disease.

Although these blood-contacting medical devices benefit millions of patients with cardiovascular disease all over the world, they are often a site of thrombosis or embolism, causing significant morbidity and mortality [4, 5]. Embolic strokes are a serious complication of MCADs [4] and thrombosis limits their use in pediatric patients. In-stent restenosis is the major complication of Nitinol stents [5]. These adverse events mandate the use of anti-platelet agents or anticoagulants, which predispose the patients to bleeding complications.

Endothelializing the blood-contacting titanium surfaces of these and other devices would provide them with an antithrombogenic and anti-inflammatory coating that mimics the native lining of blood vessels and the heart. The major limitation to this technology has been a source of easily available autologous endothelial cells that adhere under flow. Endothelial progenitor cells (EPCs) seem ideally suited to fill in this gap. The existence of putative EPCs circulating in human blood was first described by Asahara et al. in 1997 and led to a paradigm shift of the process of neovascularization in the form of postnatal vasculogenesis [6]. In subsequent years, Hill et al. isolated cells known as colony-forming unit endothelial cells (CFU-ECs) [7]. Although these cells appeared to exhibit many endothelial cell characteristics, they were subsequently found to be hematopoietic cells enriched for monocyte-macrophage or T cell lineage commitment [8]. In 2007, Yoder et al. described a peripheral blood-derived cell population referred to as endothelial colony forming cells (ECFCs) or late-outgrowth EPCs (to distinguish from early outgrowth cells, which lack proliferative potential) [8]. ECFCs display all the phenotypic and functional properties of endothelial cells but are endowed with a robust proliferative potential and the ability to form new blood vessels *in vivo*. Since ECFCs are obtainable from a simple peripheral blood draw, it should be feasible to isolate late-outgrowth EPCs from patients' own blood and coat the titanium blood-contacting surfaces with autologous cells prior to implantation. To translate such technology into clinical practice, it is desirable to seed a device within minutes before implantation and avoid precoating the surface with potentially prothrombotic proteins exposed to the blood stream (e.g. fibronectin or collagen).

We hypothesize that EPCs, derived from a peripheral blood draw, adhere well to smooth nanostructured Ti surfaces without any precoating, grow to a confluent monolayer on Ti, remain adherent and functional under physiological and supraphysiological shear stress, and endow the Ti surface with increased biocompatibility by releasing nitric oxide and inhibiting platelet adhesion.

2. Materials and methods

2.1. Titanium slide manufacturing

100 nm of Ti was deposited on piranha-cleaned glass slides (Fisher Scientific) using a CHA Industries Solution E-beam Evaporation System. The Ti purity was 99.999 %, the deposition rate was 2 Å/s, the pressure was 5×10^{-6} Torr. Slides were rotated continuously at 20 rotations per minute during the deposition process as previously described [9].

2.2. X-ray photoelectron spectroscopy

The atomic composition of our Ti samples was determined using a Kratos Axis Ultra X-ray Photoelectron Spectroscopy and compared to the inner surface of a HeartMate II MCAD adapter, provided by Thoratec as previously described [10]. Spectra were obtained at 2.0×10^{-8} Torr using a monochromated aluminum K-alpha X-ray source at a power of 15 kV and an emission current of 10 mA. Scans were performed over the range of 5–1,200 eV with a step eV of 1, a dwell time of 200 ms and a resolution of 160 eV. The surface composition of the samples was calculated from survey scans using CasaXPS software and utilizing a relative sensitivity function library specific to the Kratos Axis Ultra system.

2.3. Atomic force microscopy

Ti/ TiO₂ -coated samples were rinsed with 2 % sodium duodecyl sulfate solution followed by 30 rinses in deionized water, then dried under a stream of nitrogen, and imaged (using contact mode) in air with a V-shaped silicon nitride cantilever (Nanoprobe, Veeco, spring constant 0.12 N/m; tip radius 20-60 nm) with a MultiMode atomic force microscope (Digital Instruments) [11]. The roughness (R_q) was determined with Nanoscope 3 software according to equation (1) [12],

$$R_q = \sqrt{\frac{1}{n} \sum_{i=1}^n y_i^2} \quad (1)$$

where n is the number of measurements and y_i is the vertical distance from the calculated mean line to the i^{th} measurement.

2.4. Contact angle

The surface wettability was assessed by measuring the water contact angle at five different points per Ti slide using the sessile drop method at room temperature in air, with a drop volume of 5 μl with a Ramé-Hart NRL CA 100-00 goniometer as previously described [9].

2.5. EPC isolation

Animal care and experimentation were in accordance with the National Institute of Health Guidelines for the Care and Use of Laboratory Animals and were approved by the Duke University Institutional Animal Care and Use Committee. The animals were sedated according to protocol and femoral vein access was obtained. After discarding the first 5 ml of blood, 100-150 ml blood of five 35 kg Yorkshire swine were collected into 25 ml Citrate Phosphate Dextrose containing Cord Blood Collection Bags (Pall).

Mononuclear cells (MNCs) were collected via density centrifugation as previously described [13] and resuspended in full EPC medium (EMB-2 base medium + EGM-2 SingleQuots (Lonza) and a total of 50 ml fetal bovine serum (Hyclone)). MNCs were counted and plated at an average density of 9×10^6 MNCs per cm^2 surface area into separate wells of 6-well tissue culture plates coated with type-I rat tail collagen (BD Biosciences) at 37 °C, 5 % CO₂, in a humidified incubator. After 24 hrs of culture, nonadherent cells were removed and EPC medium was added to each well. Medium was changed daily for 7 days and then every other day following. EPC colonies formed after an average of 5-7 days. Cells were used at passages 5-10 for all experiments.

2.6. Flow cytometry

EPCs were suspended at a concentration of 1×10^6 cells/ml in 1 % bovine serum albumin in phosphate buffered saline and labeled with directly conjugated mouse anti-porcine CD14, CD45 and CD31 antibodies (Serotec MCA1746F, MCA1222F, MCA1218F). Respective isotype controls were used (Serotec MCA691F, MCA928F) and fluorescent intensity measured with a FACSCalibur flow cytometer (Becton Dickinson). For each set of samples, the fluorescent intensity of the isotype control was compared with the fluorescent intensity

of the test sample using CellQuest software (Becton Dickinson) as previously described [14].

2.7. Immunohistochemistry/ microscopy

EPC-coated Ti slides for imaging were fixed in 3.7 % formaldehyde (Ricca Chemical) and permeabilized with 0.1 % Triton X (Sigma-Aldrich). After incubation with anti-porcine CD31 (Antigenix America APG311) and anti-human eNOS (Santa Cruz) diluted 1:50, cells were stained with the secondary antibodies goat anti-rabbit AlexaFlour546 (Invitrogen), and goat anti-mouse AlexaFlour488 (Invitrogen), at 1:500 dilution [14]. Appropriate positive and negative control experiments were performed to rule out non-specific antibody binding to Ti surfaces. Nuclei were counterstained with DAPI (Vector Laboratories). To test for uptake of acetylated Low Density Lipoproteins (LDL), live cells on Ti were incubated (4 hrs, 37 °C) with DiI-labeled acetylated Low Density Lipoproteins (Biomedical Technologies).

Fluorescent microscopy was performed with an upright Leica DMRB microscope with a Qimaging Qicam monochrome digital camera and Image Pro Plus software (Leica).

2.8. Scanning electron microscopy

Samples were fixed in 3.7 % formaldehyde, dehydrated in an ethanol series, dried in a Pelco CPD2 critical point dryer (Ted Pella), and coated with Au/Pd (60/40%) in a Hummer 6.2 sputter coater (Anatech) prior to imaging. Au/Pd was sputtered from a single alloy source to a film thickness of 6-7 nm. Scanning electron microscope images were obtained with a Philips XL30 ESEM TMP (FEI Company) SEM using standard high vacuum imaging at 25 kV as described previously [10].

2.9. Redox assay

Equal numbers of EPCs were grown to a confluent monolayer on bare Ti, and glass slides precoated with bovine fibronectin (Invitrogen) (3 µg/cm² surface area) as control samples.

The alamarBlue redox assay (Invitrogen) [15] was diluted to 10% in EPC medium, added to EPC-seeded Ti and FN-glass slides (and unseeded Ti slides as control for presence of cells). The change in absorbance with respect to medium was measured with a spectrophotometer (Beckman Coulter DU 640). The percent reduction of alamarBlue by metabolizing EPCs was calculated according to manufacturer's instructions using equation (2).

$$\%Reduction = \frac{[100 \times (\epsilon_{OX}) \lambda_2 A \lambda_1 - (\epsilon_{OX}) \lambda_1 A \lambda_2]}{[(\epsilon_{RED}) \lambda_1 A' \lambda_2 - (\epsilon_{RED}) \lambda_2 A' \lambda_1]} \quad (2)$$

with (ϵ_{OX}) and (ϵ_{RED}) the molar extinction coefficient of its oxidized and reduced form, and A, A' the absorbance of the test well, negative control well, and $\lambda_1 = 570$ nm, $\lambda_2 = 600$ nm. Medium samples were obtained for analysis at the predetermined time points 0 hr, 1.5 hrs, 3.5 hrs, 6.5 hrs, 9.5 hrs and 14.5 hrs. A total of 6 experiments were performed.

2.10. Flow experiments

For all flow experiments, Ti slides were cleaned in 2 % sodium duodecyl sulfate for 30 min followed by 30 rinses in deionized water and then dried with nitrogen gas. Sterilization was achieved by steam autoclaving at 120 °C for 30 min (AMSCO Scientific Series, Gravity Stage 3).

To assess EPC adhesion under supraphysiological shear stress, EPCs were fluorescently labeled with Cell Tracker Orange (Invitrogen) (1 mM diluted in DMSO) before seeding onto bare Ti slides at a density of 20,300 cells/cm² in Quadri-PERM 4-Compartment Culture Dishes (Greiner Bio One). After a settling time of 15 min in phosphate buffered saline (PBS) at 37 °C, 5% CO₂, in a humidified incubator (NuAire), the slides were rinsed and transferred into a variable height flow chamber in a laminar flow circuit (total volume 100ml) as previously described [16] in full EPC medium. The radiopaque Ti was imaged through the transparent top of our flow chambers with an upright fluorescent microscope (Leica). 25 images (100 x magnification) were obtained in 5 predetermined positions (channel heights) and approximately 500 cells counted per position. EPCs were then exposed to shear stress calculated according to equation (3) [16], ranging from 46 dynes/cm² to 418 dynes/cm².

$$\tau = \frac{\mu Q}{wh^2} \quad (3)$$

where τ denotes the wall shear stress (dynes/cm²), μ the medium viscosity at 37 °C (0.01 gcm⁻¹s⁻¹), w is the channel width (1.8 cm), h the channel height (0.025 cm), Q the volumetric flow rate (cm³/s). After flow, images were obtained at the same positions as prior. The fraction of adherent cells was calculated as the ratio of adherent cells per position after flow to the number of adherent cells per position before flow in 14 experiments with EPCs isolated from 3 different pigs and 68 different shear stresses.

To evaluate EPC spreading under flow conditions on Ti, EPCs were seeded on Ti at densities of 200,000 cells/cm² in PBS and left to settle for 15 min, rinsed x 3 and then exposed to 15 dynes/cm². Eight experiments were conducted with EPCs derived from one of three different pigs. Images were obtained at time points 0 hr, 24 hrs and 48 hrs (at 100 x). Cell areas were determined for 500 cells per time point using Image J software and cell roundness calculated according to equation 4.

$$Roundness = \frac{4 \times \pi \times Area}{Perimeter^2} \quad (4)$$

Further, long term flow experiments at 15 dynes/cm² or 100 dynes/cm² x 48 hrs were conducted with EPCs that had been incubated x 24 hrs prior to flow on bare Ti slides (76,000 cells/cm²) in EPC medium (37 °C, 5 % CO₂). Glass slides precoated with bovine fibronectin (Invitrogen) at 0.25 µg/cm² served as control. For static control experiments, Ti slides (FN-glass slides) were incubated next to the circuit in petri dishes covered by 20 ml of EPC medium. 15 images (200 x) in 24 experiments were obtained along the axis of the slide

prior to and after flow. Areas, roundness and angels (relative to the direction of flow) were quantified for 500 cells per slide before and after flow (Image J software).

2.11. NO quantification

To quantify nitric oxide (NO) production by EPCs, we directly measured the primary oxidation product nitrite (NO_2^-) in 150 μl medium samples collected from the flow circuit reservoir and static control at 0 min, 1 hr, 6 hrs, 12 hrs, 24 hrs, 48 hrs in 24 experiments. Samples were frozen at 80°C until further analysis. The concentration of NO_2^- was measured by chemiluminescence with an Ionics/Sievers Nitric Oxide Analyzer (NOA 280, Sievers Instruments, Boulder, CO) as described previously [17]. The reductant used for nitrite analysis was potassium iodide in acetic acid (14.5 M acetic acid and 0.05 M KI), which has the reduction potential to convert nitrite to NO but is insufficient to reduce any higher oxides of nitrogen such as nitrate and thus is relatively specific for nitrite. The total amount nitrite produced was calculated as the product of concentration produced and the total volume of the circuit (100 ml) or static control (20 ml) while adjusting for volume lost while taking samples.

2.12. Platelet assay

A platelet assay previously described [18] was modified to isolate and label platelets (PLTs) prior to seeding on Ti surfaces (see Appendix for more detailed information). In order to limit PLT activation, all steps were performed with solutions on ice. To wash and suspend PLTs while minimizing PLT activation, we used a buffered saline glucose citrate solution (BSGC) containing 8.6 mM Na_2HPO_4 , 1.6 mM KH_2PO_4 , 0.12 M NaCl, 0.9 mM EDTA, 13.6 mM Na_3 Citrate, 11.1 mM Glucose, titrated to a pH of 7.1 in deionized water. All solutions were sterilized via vacuum filtration. We isolated PLTs from blood that was pooled from 4 pigs. The concentration of PLTs in solution was determined as 1.062×10^9 per ml with a Complete Blood Count Analyzer (Abbott Cell Dyn 3700 Hematology System, Abbott Diagnostics). EPCs were grown to confluency and also fluorescently labeled (1 mM solution of Cell Tracker Green). A solution of 1×10^6 PLTs labeled with Cell Tracker Orange was then suspended in a 10 ml, 1:1 solution of DMEM/Tyrodes buffer (20 mM Hepes, 137 mM NaCl, 2.7 mM KCl, 1 mM CaCl_2 , 11.9 mM NaHCO_3 , 5.5 mM Glucose) to activate PLTs. 5 ml of PLT-activating solution was added to either bare Ti or EPC-coated Ti, followed by incubation (10 min, 37°C , 5 % CO_2). Surfaces were then rinsed x 3 with PBS prior to imaging. 5 images along the Ti slide (100 x) were obtained. The experiment was repeated x 3.

2.13. Statistics

We used the mixed model (SAS, PROC MIXED) to compare the longitudinal data of alamarBlue reduction on FN-precoated glass surfaces and Ti, as well as nitric oxide production between the groups Ti or FN-glass, and high shear, physiological shear or static conditions. To compare platelet adhesion to EPC-coated and uncoated Ti we applied a T-Test (SAS, PROC TTEST). EPC spreading (area) and elongation (roundness) under flow were evaluated with the Kruskal-Wallis Test (SAS, PROC NPAR1WAY). Cell roundness between the different surfaces (Ti and FN-glass) and flow conditions (15 dynes/cm² vs. 100 dynes/cm²) was evaluated with Two-Way ANOVA (SAS, PROC GLM). The Kolmogorov-

Smirnov Test (SAS, PROC NPAR1WAY) was used to compare cell alignment under static conditions (pdf found to be uniformly distributed between 0 degree - and 90 degree angles), physiological - and supraphysiological shear stresses on Ti. The significance level was assumed to be 0.05 for all tests.

3. Results

3.1. Ti Surface composition

X-ray photoelectron spectroscopy (XPS) indicated that the chemical composition of the titanium oxide microsphere surface of the HeartMate II ventricular assist device (Thoratec) was almost identical to our manufactured Ti surfaces (Fig. 1a, b).

3.2. Ti surface topography

The topography of our Ti surfaces was assessed with atomic force microscopy (AFM). The average roughness (R_q) was approximately 10 nm (Fig. 1c). The Ti surface gave a contact angle of $42.3 \pm 1.98^\circ$ ($n = 5$), which is consistent with a Ti oxide film deposited in the absence of oxygen flow [9].

3.3. EPC isolation

Porcine EPC colonies appeared 5-7 days after isolation and had an average of 1 colony per 43 ml blood. Isolated EPCs exhibited characteristic cobblestone endothelial cell morphology by light and scanning electron microscopy (SEM) (Fig. 2a), took up DiI-labeled acetylated Low Density Lipoprotein (DiI-Ac-LDL) (Fig. 2b) and stained positive for typical endothelial cell markers such as CD31 (PECAM) (Fig. 2c), endothelial Nitric Oxide Synthase (eNOS) (Supplementary Fig. S1), Bandeiraea Simplicifolia-1 lectin, Vascular Endothelial Growth Factor-R2, and von Willebrand factor. Flow cytometry also confirmed presence of CD31 and absence of monocytic markers CD14 and CD45 (Supplementary Fig. S2).

3.4. EPC growth on Ti

The maximal seeding density of our EPCs in full EPC medium on Ti was 150,000 cells/cm². Our results indicate that EPCs attach to Ti surfaces and adhere very well when compared to fibronectin-precoated glass (FN-glass). If seeded below this density, EPCs divide and grow on Ti under static conditions until they form a confluent monolayer, fully covering the entire surface. At that point, EPCs are contact-inhibited and remain viable in long term culture on Ti (> 1 week).

3.5. EPC viability on Ti

We did not find a significant difference in metabolic activity between confluent layers of EPCs on either Ti or FN-glass surfaces in long term culture (> 1 week) using the alamarBlue redox assay (Invitrogen) ($p = 0.42$, $n = 6$) (Fig. 2d). Therefore, EPCs on uncoated Ti remain as viable as those growing on FN-glass surfaces under long term culture conditions.

3.6. Platelet adhesion

EPC-coated Ti slides and bare Ti slides (controls) were incubated for 10 min at 37 °C under identical conditions with fluorescently-labeled platelets, pooled from 4 different pigs. We found a > 500-fold difference in platelet adhesion to EPC-coated vs. uncoated surfaces ($2.5 \pm 0.3 \times 10^6$ PLTs/cm² adhered to uncoated Ti (Fig. 3a), but only 4600 ± 2000 PLTs/cm² to EPC-coated Ti (Fig. 3b), $p < 0.0001$).

3.7. EPC adhesion under shear stress

EPCs remained adherent to Ti after only 15 min settling time in saline solution without precoating of the Ti surface, even under shear stresses exceeding 20-fold normal physiological conditions, which are of the magnitude of 15-20 dynes/cm² in the human arterial system [19]. At a shear stress of approximately 200 dynes/cm², over 90 % of cells were retained on the Ti surface and at the highest shear stress of 380 dynes/cm² over 80 % of EPCs still remained adherent (Fig. 4a).

3.8. EPC spreading, retention and alignment on Ti following exposure to flow

EPCs isolated from 3 different pigs were used in separate experiments and seeded on Ti where they were left to settle in serum free medium for only 15 minutes prior to initiation of flow. EPCs spread on Ti while being subjected to continuous physiological shear stress (48 hrs) until forming a confluent monolayer (Fig. 4b-d). Their area significantly increased from $124.9 \pm 5.8 \mu\text{m}^2$ to $1524 \pm 56 \mu\text{m}^2$ after 24 hrs and to $2279 \pm 81 \mu\text{m}^2$ after 48 hrs (Fig. 4e) ($p < 0.0001$). At that time, EPCs occupied $> 96 \pm 1.2 \%$ of the Ti surface. Whereas almost perfectly round at the beginning of flow (roundness of 0.896 ± 0.004), they progressively elongated during flow (roundness = 0.63 ± 0.01 after 24 hrs, and 0.523 ± 0.00751 after 48 hrs, $p < 0.0001$, Fig. 4b-d and f).

EPCs grown to confluence on Ti x 24 hrs prior to flow and then exposed to shear stress, also maintained an intact monolayer under long term exposure (48 hrs) to physiological - (15 dynes/cm²) and supraphysiological shear stress (100 dynes/cm²). EPCs elongated under physiological shear as compared to static culture conditions (roundness = 0.688 ± 0.004 vs. 0.426 ± 0.007 , $p < 0.0001$), and even more so under supraphysiological shear stress (roundness = 0.369 ± 0.005 , $p = 0.001$) (Fig. 5a-c). Further, EPCs on Ti aligned with the direction of flow under 15 dynes/cm² (angle = $16.9 \pm 0.2^\circ$), which was significantly different from a random distribution under static conditions (angle = $44.8 \pm 0.5^\circ$, $p < 0.0001$), and even closer alignment with the direction of flow under 100 dynes/cm² (angle = $12.4 \pm 0.3^\circ$, $p < 0.0001$) (Fig. 5d).

3.9. Nitric oxide production

EPCs from 4 different pigs in 24 independent experiments produced significantly more NO during 48 hrs of physiological shear stress than during static conditions ($p < 0.0001$), and under supraphysiological shear as compared to physiological shear ($p = 0.0001$) (Fig. 5e). There was no statistically significant difference in NO production between Ti and FN-glass ($p > 0.85$).

4. Discussion

The benefit of in-vitro seeding of artificial blood-contacting surfaces with autologous endothelial cells has been demonstrated by Zilla et al. more than a decade ago, when he successfully reduced the occlusion of femoro-popliteal polytetrafluoroethylene bypass grafts [20-24]. However, all clinical utilization of this strategy was hampered by the difficulties obtaining the endothelial cells through an additional invasive procedure, such as harvesting a healthy native vessel. Other approaches to isolate cells have included isolation of EPCs from bone marrow, which requires an invasive, and painful bone marrow aspiration [25], and the culture of microvascular endothelial cells from dermal tissue. The latter has remained problematic as well, because of difficulties in isolating a pure cell population without fibroblast contamination, low endothelial cell yields, and a short lifespan of the isolated cells [26]. Since peripheral blood is readily and easily available, blood-derived EPCs may be an ideal cell type to seed onto implantable cardiovascular devices, such as Nitinol stents, which are Ti-coated, or Ti-based MCADs, as well as other blood-contacting extracorporeal devices.

In order to translate this technology into clinical practice, certain prerequisites must be met: 1. EPCs should adhere to and grow on Ti surfaces, ideally without precoating the surface with a potentially prothrombotic protein layer; 2. EPCs must adhere under shear stress on such surfaces and 3. EPCs must provide for a less thrombotic and less inflammatory surface, e.g. inhibit platelet adhesion and activation, and also release nitric oxide in analogy to healthy native endothelium.

Breithaupt et al. [27] and Yeh et al. [28] reported that human umbilical vein endothelial cells (HUVECs) can grow on Ti without surface treatment under static conditions. Our results show that blood-derived EPCs in serum-free medium adhere within minutes of seeding to non-functionalized Ti. This has the distinct advantages of avoiding activation of the coagulation cascade through exposure of prothrombotic protein coatings (collagen or fibronectin, etc.), as well as potential sensitization of the immune system against non-autologous proteins. Further, uncoated devices are easier to manufacture and less costly. Surface roughness may be an important factor for ideal EPC growth conditions and adhesion under shear stress. Chung et al. [29] compared adhesion of endothelial cells on fine grain vs. coarse grain Nitinol particles and found best results for 60 nm rather than 100 nm particles. Samaroo et al. [30] studied HUVEC adhesion to modified polyurethane surfaces of different roughness and found best adhesion for a mean roughness R_a of 35 nm. Yet, in neither study had cells been exposed to physiological shear stress. We found that the very smooth Ti surface ($R_q = 10$ nm) provides for excellent EPC adhesion under physiologic and supraphysiologic shear stresses. More than 80 % of EPCs are still retained at shear stresses 25-fold higher than physiological conditions. To the best of our knowledge, such exceptionally strong adhesion to uncoated Ti has never been reported. Only recently, similarly strong adhesion has been described for human endothelial cells and human umbilical cord blood-derived EPCs grown on smooth muscle cells [31], as well as FN-precoated surfaces [32]. We attribute this to the unique characteristics of the naturally formed titanium oxide film of Ti. Yeh et al. also found that HUVECs grow significantly better on titanium oxide as compared to other metals [28]. Further, Lin et al. recently

described an increase in cellular activity of porcine aortic smooth muscle cells as a function of increased oxygen content of Ti surfaces synthesized by electron-beam evaporation at different oxygen flow rates [9].

Given EPCs' exceptionally strong adhesion to Ti and the fact that they can spread to a monolayer under physiological flow conditions and EPCs' ability to adapt to their environment by elongating and aligning in the direction of flow, it is theoretically possible to quickly (within minutes) seed a titanium oxide-coated device immediately prior to implantation, on the operating room or catheterization laboratory table. The possibility of such quick seeding times is an important milestone to translate EPC-seeding technology into clinical practice since longer 2-step seeding procedures that require ex-vivo culture time have not proven to be practical.

Another important marker of endothelial cell functionality and health is the synthesis of NO, which also inhibits platelet adhesion in vivo [33]. However, the short half-life of NO in aqueous solutions renders it impractical for direct measurement and has led to the use of its primary oxidation products as surrogates for NO. Previous studies in human blood have shown direct measurements of plasma nitrite to be the most useful marker of vascular NO production due to its relatively low background concentrations (70-140 nM) and detection limits (< 5 pM) [34-36]. Other studies in this field have examined NOX (nitrite plus nitrate) using the Griess assay, but plasma nitrate or NOX are in the 10 μ M range in human plasma and have shown little relationship to endothelial function in vivo in humans [17]. Additionally, the Griess assay chemically converts nitrate to nitrite for measurement and has a limit of detection of 2.5 μ M in comparison to < 5 pM for the Sievers Nitric Oxide Analyzer (NOA 280, Sievers Instruments). Consequently we have selected to use the direct measurement of nitrite as a marker of NO production by our EPCs.

Since thromboemboli formation is initiated by platelet adhesion to foreign materials [37], we investigated whether an EPC-coated Ti surface would decrease platelet adhesion [38]. We chose to evaluate the propensity of platelets to adhere to EPC-coated Ti surfaces under the most extreme condition – static incubation in calcium-rich Tyrodes Buffer at 37 °C. Still, only a few platelets were observed adhering to the EPC-coated surfaces, whereas > 590-fold more platelets adhered to uncoated Ti surfaces under identical conditions.

Our study has several limitations. The interaction of EPCs (on Ti) with the native vascular environment in a stented vessel, for instance, has not been examined. Whereas we cannot rule out that EPCs would inappropriately stimulate vascular smooth muscle cell (SMC) proliferation, it seems very unlikely, given the flow mediated increase in NO production we observed and the confluent monolayer formed. The vasoprotective properties of NO have been well documented and are comparable to healthy endothelium. They include inhibition of SMC proliferation and migration [39]. Another possible limitation is that porcine EPCs may behave differently than human EPCs. However, we have already reproduced results with human EPCs from a patient with vascular disease and a healthy human volunteer (see Supplementary data). Our results pave the way for a porcine animal model, which is the most established large animal model for researching biocompatibility of implantable devices [40].

5. Conclusions

We found that it is feasible to grow blood-derived EPCs on Ti surfaces without any adsorbed proteins, that EPCs grow to a confluent monolayer on Ti under static conditions and physiological flow after only a few minutes prior adhesion time, that EPCs adhere extremely well to such surfaces, even under supraphysiological shear stresses. We have further demonstrated that EPCs on smooth Ti surfaces functionally adapt to their environment under flow, produce NO, dependent on the magnitude of shear stress stimulation, and dramatically reduce platelet adhesion when compared to uncoated Ti surfaces.

Therefore, we believe that it is feasible to quickly seed and coat Ti blood-contacting surfaces, such as Nitinol stents, mechanical assist devices and blood-contacting extracorporeal devices, with peripheral blood-derived EPCs just prior to implantation into the cardiovascular system, and thus ameliorate the common complications of platelet adhesion and thrombus formation.

Supplementary Material

Refer to Web version on PubMed Central for supplementary material.

Acknowledgments

We thank the NIH for supporting this work through Grant “Autologous EPC lining to improve biocompatibility of circulatory assist devices”, RC1HL099863-01, and the National Science Foundation Graduate Research Fellowship for its financial support of Alexandra Jantzen. Further we are indebted to Donald Pearce and Steven Owen for machining flow chambers and seeding devices, Kevin Collins for providing helpful techniques of assembling perfusion circuits and to Matt Maudsley for assisting in techniques of imaging titanium slides. We also thank Thoratec for providing HeartMate II adapter pieces and George Quick, Mike Lowe and Ianthia Parker for handling our research animals and Dr. Thomas Povsic for providing human blood samples.

References

1. Lietz K, Miller LW. Destination therapy: current results and future promise. *Semin Thorac Cardiovasc Surg.* 2008; 20(3):225–233. [PubMed: 19038733]
2. Rogers JH, Laird JR. Overview of new technologies for lower extremity revascularization. *Circulation.* 2007; 116(18):2072–2085. [PubMed: 17967988]
3. Chu CL, Wang RM, Hu T, Yin LH, Pu YP, Lin PH, et al. XPS and biocompatibility studies of titania film on anodized NiTi shape memory alloy. *J Mater Sci Mater Med.* 2009; 20(1):223–228. [PubMed: 18758918]
4. Pagani FD, Miller LW, Russell SD, Aaronson KD, John R, Boyle AJ, et al. Extended mechanical circulatory support with a continuous-flow rotary left ventricular assist device. *J Am Coll Cardiol.* 2009; 54(4):312–321. [PubMed: 19608028]
5. Schillinger M, Sabeti S, Dick P, Amighi J, Mlekusch W, Schlager O, et al. Sustained benefit at 2 years of primary femoropopliteal stenting compared with balloon angioplasty with optional stenting. *Circulation.* 2007; 115(21):2745–2749. [PubMed: 17502568]
6. Asahara T, Murohara T, Sullivan A, Silver M, van der Zee R, Li T, et al. Isolation of putative progenitor endothelial cells for angiogenesis. *Science.* 1997; 275(5302):964–967. [PubMed: 9020076]
7. Hill JM, Zalos G, Halcox JP, Schenke WH, Waclawiw MA, Quyyumi AA, et al. Circulating endothelial progenitor cells, vascular function, and cardiovascular risk. *N Engl J Med.* 2003; 348(7): 593–600. [PubMed: 12584367]

8. Yoder MC, Mead LE, Prater D, Krier TR, Mroueh KN, Li F, et al. Redefining endothelial progenitor cells via clonal analysis and hematopoietic stem/progenitor cell principals. *Blood*. 2007; 109(5):1801–1809. [PubMed: 17053059]
9. Lin Z, Lee IS, Choi YJ, Noh IS, Chung SM. Characterizations of the TiO_{2-x} films synthesized by e-beam evaporation for endovascular applications. *Biomed Mater*. 2009; 4(1):015013. [PubMed: 19075363]
10. Achneck HE, Serpe MJ, Jamiolkowski RM, Eibest LM, Craig SL, Lawson JH. Regenerating titanium ventricular assist device surfaces after gold/palladium coating for scanning electron microscopy. *Microsc Res Tech*. 2010; 73(1):71–6. [PubMed: 19642216]
11. Chen T, Zhang J, Chang DP, Garcia A, Zauscher S. Fabrication of micro-patterned stimulus-responsive polymer brush ‘anemones’. *Advanced Materials*. 2009; 21(18):1825–1829.
12. DeGarmo, PE.; Black, JT.; Kohser, RA. *Materials and processes in manufacturing*. 9th ed. Wiley; 2003. p. 223materials and processes in manufacturing
13. Broxmeyer HE, Srour E, Orschell C, Ingram DA, Cooper S, Plett PA, et al. Cord blood stem and progenitor cells. *Methods Enzymol*. 2006; 419:439–473. [PubMed: 17141066]
14. Stroncek JD, Grant BS, Brown MA, Povsic TJ, Truskey GA, Reichert WM. Comparison of endothelial cell phenotypic markers of late-outgrowth endothelial progenitor cells isolated from patients with coronary artery disease and healthy volunteers. *Tissue Eng Part A*. 2009; 15(11): 3473–3486. [PubMed: 19435420]
15. Fields RD, Lancaster MV. Dual-attribute continuous monitoring of cell proliferation/cytotoxicity. *Am Biotechnol Lab*. 1993; 11(4):48–50. [PubMed: 7763491]
16. Bhat VD, Truskey GA, Reichert WM. Fibronectin and avidin-biotin as a heterogeneous ligand system for enhanced endothelial cell adhesion. *J Biomed Mater Res*. 1998; 41(3):377–385. [PubMed: 9659606]
17. Allen JD, Miller EM, Schwark E, Robbins JL, Duscha BD, Annex BH. Plasma nitrite response and arterial reactivity differentiate vascular health and performance. *Nitric Oxide*. 2009; 20(4):231–237. [PubMed: 19371597]
18. Baker GR, Sullam PM, Levin J. A simple, fluorescent method to internally label platelets suitable for physiological measurements. *Am J Hematol*. 1997; 56(1):17–25. [PubMed: 9298862]
19. Truskey, GA.; Yuan, F.; Katz, DF. Rheology and flow of blood. In: Horton, MJ., editor. *transport phenomena in biological systems*. Pearson Education, Inc.; Upper Saddle River, New Jersey: 2004. p. 103-105.07458
20. Zilla P, Deutsch M, Meinhart J, Puschmann R, Eberl T, Minar E, et al. Clinical in vitro endothelialization of femoropopliteal bypass grafts: an actuarial follow-up over three years. *J Vasc Surg*. 1994; 19(3):540–548. [PubMed: 8126869]
21. Leseche G, Ohan J, Bouttier S, Palombi T, Bertrand P, Andreassian B. Above-knee femoropopliteal bypass grafting using endothelial cell seeded PTFE grafts: five-year clinical experience. *Ann Vasc Surg*. 1995; 9(Suppl):S15–23. [PubMed: 8688305]
22. Magometschnigg H, Kadletz M, Vodrazka M, Dock W, Grimm M, Grabenwoger M, et al. Prospective clinical study with in vitro endothelial cell lining of expanded polytetrafluoroethylene grafts in crural repeat reconstruction. *J Vasc Surg*. 1992; 15(3):527–535. [PubMed: 1538510]
23. Deutsch M, Meinhart J, Fischlein T, Preiss P, Zilla P. Clinical autologous in vitro endothelialization of infrainguinal ePTFE grafts in 100 patients: a 9-year experience. *Surgery*. 1999; 126(5):847–855. [PubMed: 10568184]
24. Meinhart J, Deutsch M, Zilla P. Eight years of clinical endothelial cell transplantation. closing the gap between prosthetic grafts and vein grafts. *Asaio J*. 1997; 43(5):M515–521. [PubMed: 9360096]
25. Reyes M, Dudek A, Jahagirdar B, Koodie L, Marker PH, Verfaillie CM. Origin of endothelial progenitors in human postnatal bone marrow. *J Clin Invest*. 2002; 109(3):337–346. [PubMed: 11827993]
26. Richard L, Velasco P, Detmar M. A simple immunomagnetic protocol for the selective isolation and long-term culture of human dermal microvascular endothelial cells. *Exp Cell Res*. 1998; 240(1):1–6. [PubMed: 9570915]

27. Breithaupt-Faloppa AC, de Lima WT, Oliveira-Filho RM, Kleinheinz J. In vitro behaviour of endothelial cells on a titanium surface. *Head Face Med.* 2008; 4:14. [PubMed: 18651979]
28. Yeh HI, Lu SK, Tian TY, Hong RC, Lee WH, Tsai CH. Comparison of endothelial cells grown on different stent materials. *J Biomed Mater Res A.* 2006; 76(4):835–841. [PubMed: 16345092]
29. Chung TW, Liu DZ, Wang SY, Wang SS. Enhancement of the growth of human endothelial cells by surface roughness at nanometer scale. *Biomaterials.* 2003; 24(25):4655–4661. [PubMed: 12951008]
30. Samaroo HD, Lu J, Webster TJ. Enhanced endothelial cell density on NiTi surfaces with sub-micron to nanometer roughness. *Int J Nanomedicine.* 2008; 3(1):75–82. [PubMed: 18488418]
31. Wallace CS, Champion JC, Truskey GA. Adhesion and function of human endothelial cells co-cultured on smooth muscle cells. *Ann Biomed Eng.* 2007; 35(3):375–386. [PubMed: 17191127]
32. Brown MA, Wallace CS, Angelos M, Truskey GA. Characterization of umbilical cord blood-derived late outgrowth endothelial progenitor cells exposed to laminar shear stress. *Tissue Eng Part A.* 2009; 15(11):3575–3587. [PubMed: 19480571]
33. Achneck HE, Sileshi B, Lawson JH. Review of the biology of bleeding and clotting in the surgical patient. *Vascular.* 2008; 16(Suppl 1):S6–13. [PubMed: 18544308]
34. Lauer T, Preik M, Rassaf T, Strauer BE, Deussen A, Feelisch M, et al. Plasma nitrite rather than nitrate reflects regional endothelial nitric oxide synthase activity but lacks intrinsic vasodilator action. *Proc Natl Acad Sci U S A.* 2001; 98(22):12814–12819. [PubMed: 11606734]
35. Allen JD, Cobb FR, Gow AJ. Regional and whole-body markers of nitric oxide production following hyperemic stimuli. *Free Radic Biol Med.* 2005; 38(9):1164–1169. [PubMed: 15808413]
36. Kleinbongard P, Dejam A, Lauer T, Rassaf T, Schindler A, Picker O, et al. Plasma nitrite reflects constitutive nitric oxide synthase activity in mammals. *Free Radic Biol Med.* 2003; 35(7):790–796. [PubMed: 14583343]
37. Arvidsson S, Askendal A, Tengvall P. Blood plasma contact activation on silicon, titanium and aluminium. *Biomaterials.* 2007; 28(7):1346–1354. [PubMed: 17156838]
38. Thor A, Rasmusson L, Wennerberg A, Thomsen P, Hirsch JM, Nilsson B, et al. The role of whole blood in thrombin generation in contact with various titanium surfaces. *Biomaterials.* 2007; 28(6):966–974. [PubMed: 17095084]
39. Zuckerbraun BS, Shiva S, Ifedigbo E, Mathier MA, Mollen KP, Rao J, et al. Nitrite potently inhibits hypoxic and inflammatory pulmonary arterial hypertension and smooth muscle proliferation via xanthine oxidoreductase-dependent nitric oxide generation. *Circulation.* 121(1):98–109. [PubMed: 20026772]
40. Kang C, Bonneau M, Brouland JP, Bal dit Sollier C, Drouet L. In vivo pig models of venous thrombosis mimicking human disease. *Thromb Haemost.* 2003; 89(2):256–263. [PubMed: 12574804]

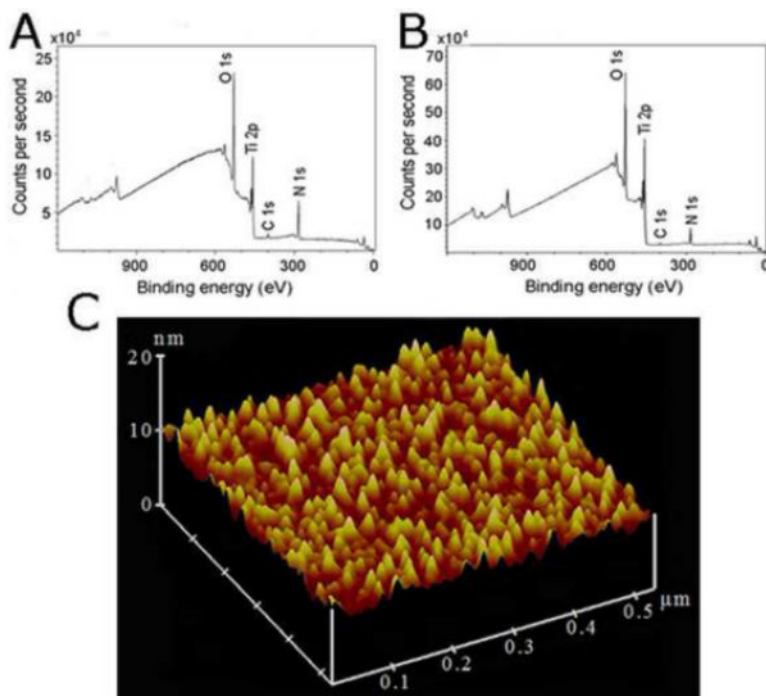


Fig. 1. (a) Representative XPS spectrum of the HeartMate II Ti inner surface (14 % Ti, 43 % O₂, 41 % C, 2 % N). (b) XPS spectrum of Ti-coated slides prepared according to the Materials and Methods (22 % Ti, 52 % O₂, 23 % C, 2 % N). The carbon atom peaks and small nitrogen atom peaks in the XPS spectra reflect contaminations from the environment on the surfaces [10]. (c) Atomic force microscopy image of our Ti surface topography.

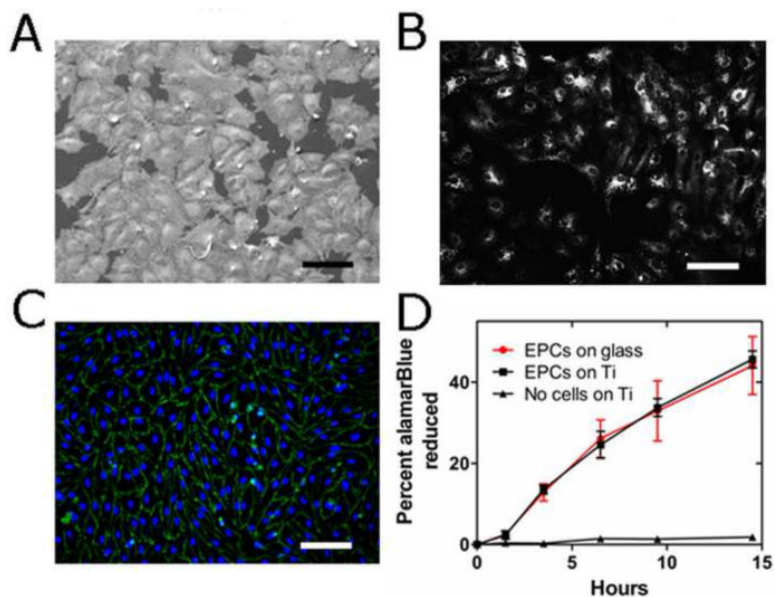


Fig. 2.

(a) SEM image of EPCs on Ti surface. (b) EPCs on Ti take up DiI-Ac-LDL. (c) EPCs on Ti stained for CD31 (green). Nuclei stained with DAPI (blue). Scale bar = 100 μm for A, B, C. (d) EPCs' metabolic activity measured via the surrogate % reduction of the alamarBlue assay after long term culture (> 1week) on either FN-glass surfaces (red) or Ti surfaces (black). No significant difference was observed over the course of 14.5 hrs ($p = 0.42$, $n = 6$, mixed model).

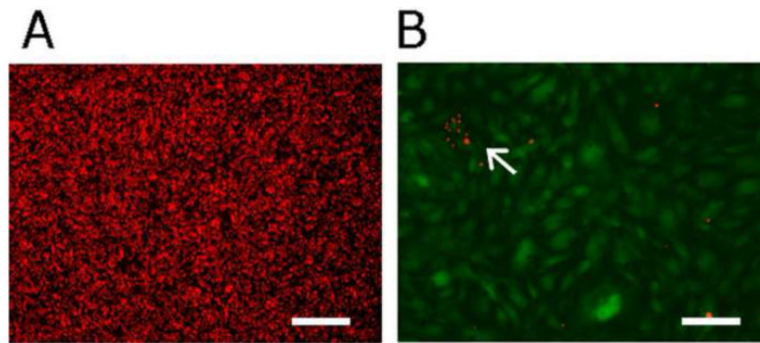
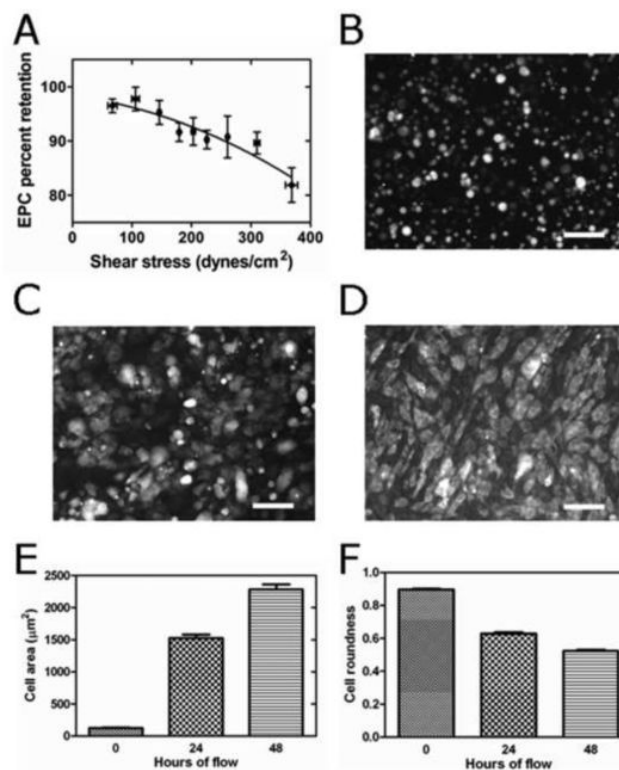


Fig. 3. Platelets labeled with Cell Tracker Orange and incubated under identical conditions in a 1:1 solution of DMEM/ Tyrodes Buffer (followed by 3 washes with buffered saline) on (a) bare Ti and (b) EPC-coated Ti (Cell Tracker Green). White arrow points toward group of PLTs on EPC-coated Ti. A > 590-fold difference in platelet adhesion was observed in 5 images per slide and 3 independent experiments ($p < 0.0001$). Scale bar = 100 μm for both images.

**Fig. 4.**

(a) % EPC retention under 68 different (increasing) shear stresses after 15 min settling time on Ti followed by 5 min flow. Results grouped into 9 clusters. For each shear stress, 5 images at 100 x magnification with approximately 100 cells per image were evaluated. EPCs were derived from 3 different pigs. Error bars indicate ± 1 SEM. (b) EPCs on Ti at initiation of flow, (c) 24 hrs, and (d) 48 hrs after initiation of flow at 15 dynes/cm². Area (e) and roundness (f) of EPCs on Ti after 0 hr, 24 hrs and 48 hrs of flow at 15 dynes/cm². Error bars indicate ± 1 SEM for E,F.

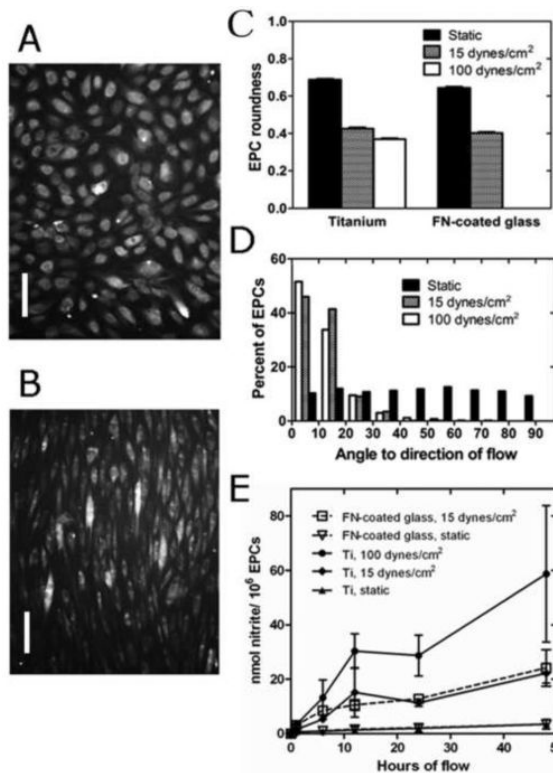


Fig. 5.

(a) EPCs on Ti after 24 hrs culture and stained with Cell Tracker Orange. (b) Same field of view after 48 hrs flow at 100 dynes/cm². Scale bar = 100 μm for both images. (c) Roundness of EPCs on Ti and FN-glass under static conditions, 15 dynes/cm² and 100 dynes/cm² shear stress. EPCs on Ti significantly elongated under 15 dynes/cm² ($p < 0.0001$, $n = 500$ cells per group, 2-Way ANOVA) and more so under 100 dynes/cm² ($p = 0.001$, $n = 500$ cells per group, 2-Way ANOVA). (d) The angle frequency distribution of EPCs on Ti at 15 dynes/cm² x 48 hrs is significantly different from static conditions ($p < 0.0001$, $n = 500$ angles per group, KS-Test) and shear stress at 100 dynes/cm² x 48 hrs ($p < 0.0001$, $n = 500$ angles per group, KS-Test). (e) Amount of nitrite (nmol) produced per 1 $\times 10^6$ EPCs as a surrogate for NO synthesized on Ti (solid lines) or FN-glass (interrupted lines) surfaces. Nitrite production was significantly larger under 15 dynes/cm² than under static conditions ($p < 0.0001$), and under 100 dynes/cm² as compared to 15 dynes/cm² ($p = 0.0001$), but not different between Ti and FN-glass surfaces ($p = 0.859$). $N = 24$ experiments, mixed model.